Korean J. Chem. Eng., **28**(8), 1684-1687 (2011)
DOI: 10.1007/s11814-011-0045-1

Effect of CdS contents on H_2 production from Pt-(CdS/TiO_2) film-typed photocatalysts

Eunpyo Hong, Jin Hyun Kim, Sunhye Yu, and Jung Hyeun Kim†

Department of Chemical Engineering, University of Seoul, 90 Jeonnong-dong, Dongdaemun-gu, Seoul 130-743, Korea
(*Received 18 January 2011 • accepted 21 February 2011*)

Abstract−Pt-(CdS/TiO_2) film-typed photocatalysts are prepared with a doctor-blade method followed by a chemical bath deposition (CBD) process, and the films are characterized by UV-vis spectroscopy, scanning electron microscopy, energy-dispersive X-ray spectroscopy. The film-typed structure is composed of photocatalysts and Pt metal part on a FTO substrate without additional electric device, so it is relatively simpler than the conventional photoelectrochemical cell. CdS quantum dots are introduced as a sensitizer for visible light response. Amounts of CdS quantum dots on TiO_2 surface are increased with increasing CBD cycles, but they start to aggregate after certain CdS concentration due to oversaturation phenomenon. This high CdS content induces high electron losses, and therefore it reduces amounts of hydrogen production. As a result, there is a saturation point of CdS content at Cd/Ti ratio of 0.197, and the amounts of evolved hydrogen are 5.407 μmol/cm^2·h at this photocatalyst formulation.

Key words: Hydrogen Production, Photocatalyst, Titanium Dioxide, Cadmium Sulfide, Chemical Bath Deposition

INTRODUCTION

Hydrogen production by water splitting mechanism with solar energy source is promising because of its advantageous characteristics: abundant, environmental, and sustainable. Hydrogen is considered as a clean energy alternative since it leaves only water after usage with oxygen. Electrochemical photolysis of water was first developed by Fujishima et al. [1] in 1972; after their study many researchers reported results on photocatalytic activities of materials [2-5]. Especially, TiO_2 photocatalyst materials have been widely used in various applications due to high corrosion resistance, high reactivity to UV light, and easy availability. However, TiO_2 itself has relatively low photocatalytic activity for hydrogen production because of the large band-gap (3.2 eV, anatase), rapid electron-hole recombination, and fast reverse reaction to H_2O. To overcome these problems, many researchers have studied various approaches such as transition metal doping [6], metal loading [7], composite semiconductor [8,9], sacrificial agent [10], dye [11,12] and so on. Among these techniques, composite semiconductor approach is very useful for expanding the photo-reaction region into visible-light for increasing electron generation from a conjugation material which has smaller band-gap than the base materials. Besides, excited electron-hole pair by solar irradiation is stably separated without recombination process. Therefore, composite semiconductor approach can resolve the major drawbacks of TiO_2 photocatalyst in hydrogen production. As conjugation materials with TiO_2, several types of semiconductors such as CdS [8,9], CdSe and CdTe [13], CuO and Al_2O_3 [14] have been studied. In this study, we used a CdS quantum dot for conjugation material because it is the most suitable sensitizer for TiO_2 considering the magnitude of band-gap energy, positions of conduction band and valence band.

†To whom correspondence should be addressed.
E-mail: jhkimad@uos.ac.kr

Hydrogen production methods using photocatalysts can be categorized into two cases. The first, the PEC (photoelectrochemical) cell, consists of photocatalysts and counter-electrode, and they are connected with an electric wire. The second one consists of only photocatalysts itself without any electrical connection, for example particle-typed photocatalyst. In the second case, some of the film-typed photocatalysts have also been reported on metal substrates such as Ti, Zr, Al, and Fe. Kitano et al. [15] studied the effect of substrates on hydrogen production and demonstrated that the photocatalytic activity increased significantly with a decrease in work functions of the metal substrates. In using metal substrates, the cost of substrates is a challenging problem.

In this study, film-type photocatalyst in the second case was used because it is a much simpler system than the conventional PEC cell, and the film-type system was composed of photocatalysts conjugated with CdS quantum dots and Pt metal part on FTO glass without electric wire. We used an FTO glass as a conducting substrate because FTO glass is relatively cheap and good for manufacturing a TiO_2 photocatalyst film by a doctor-blade method from liquid phase.

EXPERIMENTAL

1. Preparation of the Photocatalysts and Characterization

All materials were from Aldrich unless otherwise specified and used without further purification. Commercial nanocrystalline titanium dioxide was Degussa P25. Fluorine-doped tin oxide (FTO, about 6-9 Ω/cm^2, Pilkington) was used as a transparent conducting oxide substrate for preparing TiO_2 meso-porous films. For this purpose, FTO electrodes were cut to make sample slides of 3 cm×6 cm (18 cm^2). It was carefully cleaned by ethanol after sonication. 67% area of the substrate was used for photocatalyst and the other was used for the Pt metal film. Doctor-blade method was used for fabricating the TiO_2 mesoporous film. TiO_2 paste was formed with TiO_2 (P25) 5 g, polyethylene oxide 1.25 g of molecular weight of 10^5 g/

mol, deionized (DI) water 25 g, acetyl acetone 0.1 mL. After the doctor-blade process for attachment of TiO_2 film onto an FTO substrate, the film was sintered at 500 °C for 30 min. For synthesizing CdS quantum dots, the CBD process steps were used as previously reported by other researchers [16-18]. Briefly, the TiO_2 film was immersed for 5 min in a 0.1 M $Cd(CH_3COO)_2 \cdot 2H_2O$ aqueous solution and rinsed with DI water. Then it was immersed for another 5 min in a 0.1 M $Na_2S \cdot 9H_2O$ aqueous solution and rinsed again with DI water. The full CBD cycle consists of those two step immersions. The Pt metal film was also deposited on the FTO glass using 0.7 mM $H_2PtCl_6 \cdot 6H_2O$ in 2-propanol solution, and it was also sintered at 500 °C for 20 min.

For the characterization of photocatalysts, diffuse reflectance UV-vis absorbance spectra, scanning electron microscopy (SEM) and energy-dispersive X-ray spectroscopy (EDS) were used. UV-vis (Scinco, S-4100) spectra identified the photo response region of photocatalysts. SEM and EDS (Carl Zeiss, Supra 55VP) were used to confirm morphology and distribution of CdS quantum dots through photocatalyst film.

2. Photocatalytic Reaction

The reactor was cylindrical with total volume of 330 mL and it was made of Pyrex glass. Pyrex glass cuts off wavelengths below 300 nm. Before experiment, the reactor was deaerated with N_2 gas for about 1 hour. For hydrogen production, photocatalytic reactions were carried out in 150 mL 0.40 mM $Na_2S \cdot 9H_2O$ aqueous solution. The film-type photocatalysts were immersed into solution and continuously stirred. A solar simulator (Peccell Technologies, PEC-L11) with 150 W Xe lamp and AM 1.5G filter was used as a light source and its intensity was 1,000 W/m^2 (top side irradiation). Evolved gas was collected every 30 min with gas-tight syringe and analyzed by a gas chromatograph (Chrompack, CP9001).

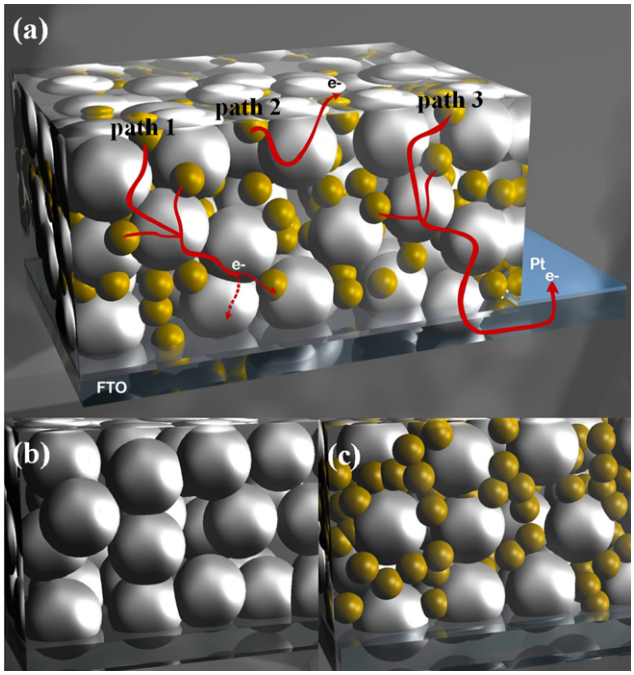

Fig. 1. Schematic views of the film-typed photocatalysts: (a) CdS saturated film showing three possible electron pathways, (b) no CdS added, (c) CdS oversaturated.

RESULTS AND DISCUSSION

1. Schematic View and UV-vis Diffuse Reflectance Spectra

A schematic view of the film-typed photocatalyst on the FTO glass is shown in Fig. 1. Fig. 1(a) shows a photocatalyst film with CdS saturated structure including three different electron pathways: 1) electrons dissipated inside the photocatalyst film, 2) electrons consumed by reactions at the photocatalyst surface, 3) electrons transferred to the Pt electrode. Amongst three possible electron paths, the third one is the most effective for hydrogen production like a PEC cell within the same substrate. Fig. 1(b) shows the mesoporous TiO_2 film formed by sintering process without CdS quantum dots, and Fig. 1(c) is a CdS oversaturated structure on sintered mesoporous TiO_2 film.

Fig. 2 shows UV-vis absorbance spectra, and the absorption edge shifts to red with increasing CBD cycles due to the increased amount of CdS quantum dots. The shape of the absorbance spectrum is

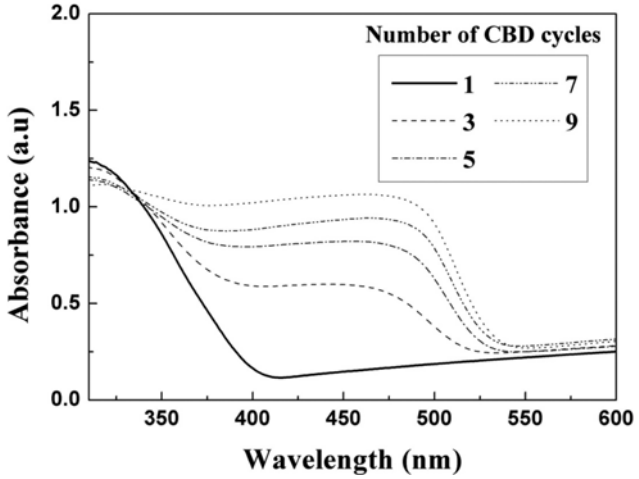

Fig. 2. Diffuse reflectance UV-vis absorbance spectra as a function of CBD cycles.

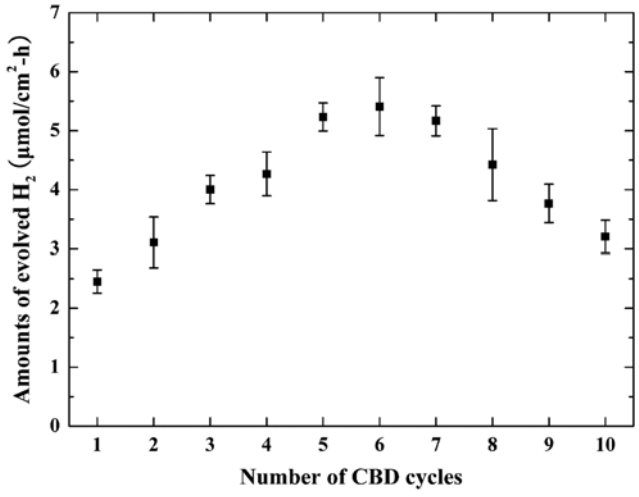

Fig. 3. Amounts of evolved hydrogen as a function of CBD cycles. Each symbol represents the average amounts of evolved hydrogen from three independent measurements including standard deviations.

changed with increasing CBD cycles, and it is possibly attributed to the relative effect of CdS content on visible light interactions. It is expected that the increased absorbance in visible light region will enhance electron excitations under solar irradiation. Absorbance spectra were indirectly measured from reflectance data, and slight increase of the absorbance in visible region possibly resulted from the reduced reflectance due to increased transmittance.

2. Photocatalytic Hydrogen Evolution

Fig. 3 shows the amounts of hydrogen produced by the photocatalytic reaction as a function of the number of CBD cycles. Amounts of the evolved hydrogen were linearly increased within our experimental range of reaction time (2.5 hrs), so 2.5 hrs reaction time was used for measurements of the evolved hydrogen. The maximum amount of hydrogen was evolved at the six-times of the CBD cycles. The CdS quantum dots were continuously increased with increasing CBD cycles as explained above in Fig. 2 with UV-vis absorbance spectra. Amounts of the CdS nanoparticles were not saturated before six-times of CBD cycles, so electrons produced by CdS sites can effectively move to the Pt metal part. However, CdS oversaturation would be the major reason of decreasing the amounts of evolved hydrogen because it could increase the electron loss by pathway 1) in Fig. 1(a). In CdS oversaturation, the CdS crystals are aggregating themselves not onto TiO_2 (Fig. 1(c)). Similar phenomena were also reported in previous investigations [19,20] with a quantum dot solar cell. Baker et al. [20] explained this phenomenon as CdS dots are aggregated until growing its size about 20 nm (in our study, the primary size of CdS nanoparticle is about 5-7 nm, measured by transmission electron microscopy), so it causes high electron losses. Therefore, the optimum amount of CdS quantum dots was achieved at six-times of CBD cycles in this study, and the maximum amount of evolved hydrogen was 5.407 μmol/cm^2·h at this condition.

In addition, we examined the effect of surface reaction by the electron pathway 2. The photocatalyst structure was modified by removing the Pt metal part from Fig. 1(a), so the possibility of pathway 2 reaction could be increased. We prepared photocatalyst film (dimension is 3 cm×4 cm) without Pt metal part, and negligible amount of evolved hydrogen was produced through the pathway 2. Therefore, it is believed that the most amount of evolved hydrogen could be generated through the pathway 3 as shown in Fig. 1(a).

3. SEM/EDS Analysis

To identify distributions of the CdS quantum dots through the photocatalyst films, the EDS was used. It is a useful technique to analyze elemental components in samples, and element maps can be obtained. Fig. 4 shows an SEM image of a cross-sectional view of the photocatalyst film and elemental analysis results (line profile and mapping data). Fig. 4(a) represents a typical morphology of the photocatalyst film. Fig. 4(b) shows the CdS distributions with color mapping (Cd: green and Ti: red) as a function of the CBD cycles. The CdS quantum dots were well dispersed in TiO_2 film, and the concentrations increased with increasing the number of the CBD cycles. Fig. 4(c) is an example plot of the line profile from the six-times of the CBD cycles. Measurements for the line profile analysis were performed across the fractured film surface as indicated with an arrow in Fig. 4(a). The total mass for the line profile analysis is measured assuming only Ti and Cd elements present. The relative mass ratios of the Cd and Ti components for all CBD cycles were calculated based on the line profile analysis, and are summarized in Table 1. The highest amount (Fig. 3) of hydrogen from the Pt-(CdS/TiO_2) film-typed photocatalyst was produced at

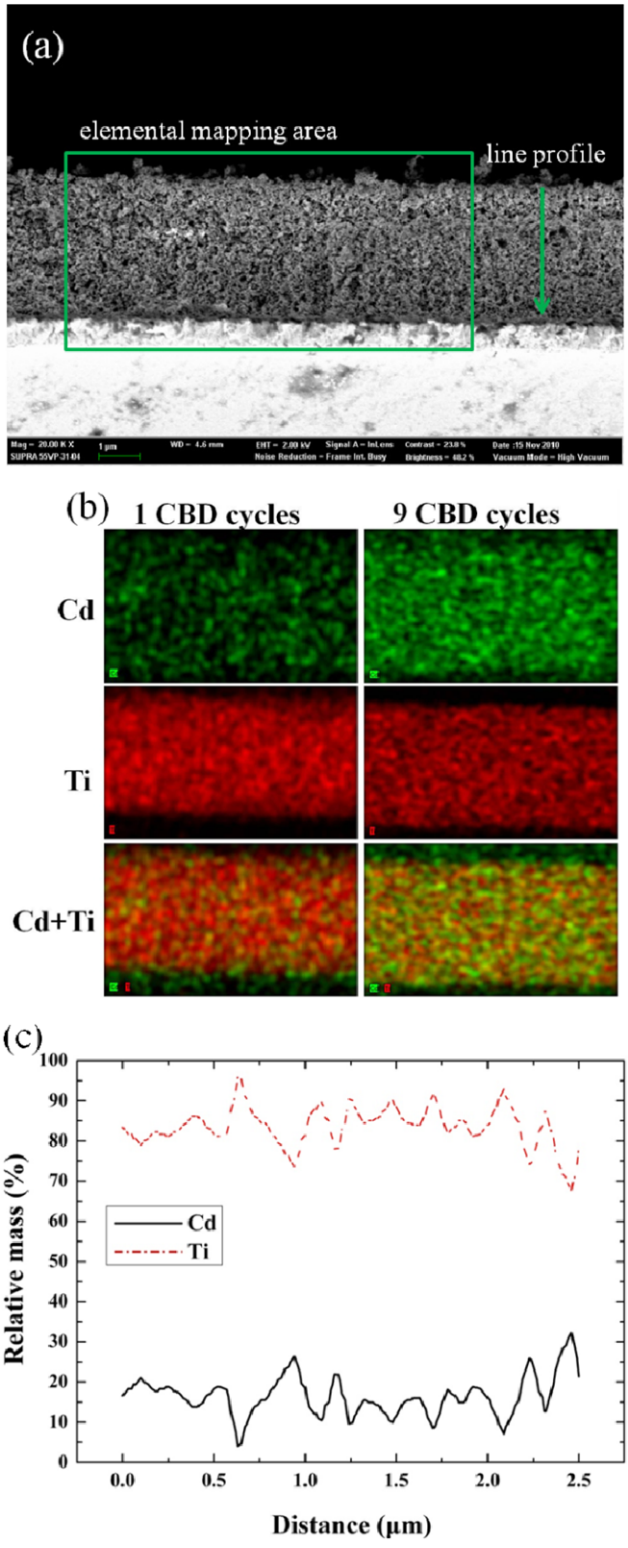

Fig. 4. Photocatalyst film structure and element distributions: (a) SEM image of the film on a FTO substrate, (b) elemental mapping data for CdS distributions with color mapping (Cd: green and Ti: red), (c) EDS line profile data for Cd/Ti relative mass from 6 CBD cycles.

Table 1. Relative mass ratio of the Cd and Ti elements for various CBD cycles

Ratio	Number of CBD cycles									
	1	2	3	4	5	6	7	8	9	10
Cd/Ti	0.009	0.064	0.103	0.114	0.155	0.197	0.252	0.301	0.365	0.378

Cd/Ti ratio of 0.197 with six-times of CBD cycles, and it is believed as the saturation point of CdS quantum dots for our film structure.

CONCLUSIONS

Pt-(CdS/TiO_2) film-typed photocatalyst has a structural advantage over a conventional PEC cell system. The CdS quantum dots were introduced into TiO_2 films in order to utilize visible light from solar irradiation for photocatalytic response. They were synthesized with a CBD process, and the amounts of CdS crystals increased with increasing the number of the CBD cycles. The amounts of evolved hydrogen also varied with the CdS contents, and the optimal CdS content in the Pt-(CdS/TiO_2) film-typed photocatalyst was obtained for hydrogen production. The highest amount of evolved hydrogen was 5.407 μmol/cm^2·h at six-times of CBD cycles, and the Cd/Ti ratio was measured as 0.197 with the EDS line profile analysis. The high amounts of CdS nanoparticles in the photocatalyst film after six-times of CBD cycles would rather promote electron losses due to the CdS oversaturation, so amounts of evolved hydrogen decreased after the saturation point of CdS quantum dots.

ACKNOWLEDGEMENTS

This work was partially supported by a grant (Code No. 2010T100200196) from Korea Institute of Energy Technology Evaluation and Planning under the Energy R&D Programs of the Ministry of Knowledge and Economy, Korea. It is also partially supported by a grant (Code No. 201003102001) from Korea Foundation for the Advancement of Science and Creativity.

REFERENCES

1. A. Fujishima and K. Honda, *Nature*, **238**, 37 (1972).
2. S. Lee, C. Yun, M. Hahn, J. Lee and J. Yi, *Korean J. Chem. Eng.*, **25**, 892 (2008).
3. I. Kim, H. Ha, S. Lee and J. Lee, *Korean J. Chem. Eng.*, **22**, 382 (2005).
4. K. Domen, M. Hara, J. Kondo, T. Takata, A. Kudo, H. Kobayashi and Y. Inoue, *Korean J. Chem. Eng.*, **18**, 862 (2001).
5. S. Lee and H. Lee, *Korean J. Chem. Eng.*, **15**, 463 (1998).
6. H. Luo, T. Takata, Y. Lee, J. Zhao, K. Domen and Y. Yan, *Chem. Mater.*, **16**, 846 (2004).
7. G. Bamwenda, S. Tsubota, T. Nakamura and M. Haruta, *J. Photochem. Photobiol. A: Chem.*, **89**, 177 (1995).
8. H. Park, W. Choi and M. Hoffmann, *J. Mater. Chem.*, **18**, 2379 (2008).
9. H. Tada, T. Mitsui, T. Kiyonaga, T. Akita and K. Tanaka, *Nature Mater.*, **5**, 782 (2006).
10. H. Liu, J. Yuan and W. Shangguan, *Energy Fuels*, **20**, 2289 (2006).
11. T. Peng, D. Ke, P. Cai, K. Dai, L. Ma and L. Zan, *J. Power Sources*, **180**, 498 (2008).
12. T. Sreethawong, C. Junbua and S. Chavadej, *J. Power Sources*, **190**, 513 (2009).
13. J. Bang and P. Kamat, *ACS Nano*, **3**, 1467 (2009).
14. T. Miwa, S. Kaneco, H. Katsumata, T. Suzuki, K. Ohta, S. Chand Verma and K. Sugihara, *Int. J. Hydrog. Energy*, **35**, 6554 (2010).
15. M. Kitano, K. Tsujimaru and M. Anpo, *Appl. Catal. A: Gen.*, **314**, 179 (2006).
16. S. Lin, Y. Lee, C. Chang, Y. Shen and Y. Yang, *Appl. Phys. Lett.*, **90**, 143517 (2007).
17. N. Strataki, M. Antoniadou, V. Dracopoulos and P. Lianos, *Catal. Today*, **151**, 53 (2010).
18. Y. Lee, C. Chi and S. Liau, *Chem. Mater.*, **22**, 922 (2009).
19. R. Vogel, K. Pohl and H. Weller, *Chem. Phys. Lett.*, **174**, 241 (1990).
20. D. Baker and P. Kamat, *Adv. Funct. Mater.*, **19**, 805 (2009).